

# Polycytosine regions contained in DNA hairpin loops interact via a four-stranded, parallel structure similar to the i-motif

Jan Rohozinski\*, John M. Hancock<sup>+</sup> and Max A. Keniry<sup>1</sup>

Research School of Biological Sciences and <sup>1</sup>Research School of Chemistry, Australian National University, Canberra, ACT 0200, Australia

Received July 22, 1994; Revised and Accepted October 10, 1994

## ABSTRACT

**Thermal denaturation profiles of an oligodeoxynucleotide that forms a hairpin structure with a cytidine-rich loop show an unexpected transition at 60°C at pH 5.0 but not at pH 8.0. Analytical ultracentrifugation shows that this transition reflects dimer formation via the interaction of loops from two molecules to form a novel structure termed the h-dimer. The dependence of this structure on low pH implies the formation of cytosine – protonated cytosine base pairs. NMR spectroscopy, thermal denaturation and ultraviolet absorption spectral analysis suggest a similarity to the i-motif structure recently proposed for the interaction of deoxycytidine oligomers. The use of hairpin loops to form i-motif-like structures may prove useful in searches for cognate proteins and possibly in the production of antibodies.**

## INTRODUCTION

In recent years there has been renewed interest in the tertiary structures formed by nucleic acids. Much effort has been directed at discriminating between the various forms of DNA with the goal of understanding the *in vivo* significance of DNA tertiary structure and possibly one day harnessing that knowledge for therapeutic purposes. Recent interest in DNA quadruplexes has revealed an array of diverse structural forms (1–3). The most recent and surprising is a novel four stranded structure formed by polydeoxycytidine at acid pH (4,5). This structure, termed the i-motif, involves the interdigitation of two pairs of oligonucleotides with each pair consisting of two strands of oligodeoxycytidine running parallel and pairing by way of cytosine – protonated cytosine (C.C<sup>+</sup>) base pairs (Fig. 1A) (4,5). This tetrameric structure differs significantly in its properties from the previously accepted duplex model (5). It also differs from triple helical structures in not requiring cations for stability (6). Furthermore, in contrast to a triple helix in which all three DNA or RNA strands are held together by hydrogen bonds (6) the i-

motif is stabilised by alternate stacking of C.C<sup>+</sup> base pairs (4,5,7).

While investigating the thermodynamic and spectral properties of DNA hairpin loops an unexpected interaction has been observed at low but not neutral pH between hairpin molecules containing cytidine-rich loops. Because of structural constraints imposed by the presence of the stem region of the hairpin, and the fact that the interaction was only observed at acid pH, it was hypothesised that C.C<sup>+</sup> base pairing was responsible for the interaction. Since stable C.C<sup>+</sup> bonds cannot form between poly(C) strands running antiparallel it was further hypothesised that two hairpins were interacting via poly(C) tracts lying parallel to form an i-motif-like structure, which we term the h-dimer (hairpin-dimer). Presence of the i-motif in these structures is supported by NMR spectroscopy and dimer formation demonstrated by analytical ultracentrifugation.

## MATERIALS AND METHODS

### Oligodeoxynucleotides

Two oligodeoxynucleotides were used in this study. The oligodeoxynucleotide 5'-GCATCGTTCCCCCCCCCTCTC-TCCCCCCCCTTCGATGC-3' (here designated CL) can form a stem – loop structure that includes two opposed eight nucleotide cytosine tracts (Fig. 1A). 5'-CCCCCCCC-3' (C<sub>8</sub>) was used as a positive control for i-motif formation at low pH (4). Oligodeoxynucleotides were purified by HPLC to ensure correct length and stored frozen (–18°C) in water solution. Solutions for subsequent analysis were prepared on ice.

### Thermal denaturation

Comparative thermal denaturation studies were carried out between CL and C<sub>8</sub> at pH 5.0 and pH 8.0. Thermal denaturation was carried out in 300 μl volumes in a Gilford Thermo-Programmer 2527 cell mounted in a Gilford 250 spectrophotometer. Oligodeoxynucleotides were dissolved in 0.1 M sodium acetate, 10 mM NaCl, pH 5.0 or 8.0, in the presence

\*To whom correspondence should be addressed

<sup>+</sup>Present address: MRC Clinical Sciences Centre, Royal Postgraduate Medical School, Hammersmith Hospital, DuCane Road, London W12 0NN, UK

or absence of 10 mM MgCl<sub>2</sub>. Thermal denaturation was carried out at a concentration of 1 μM oligodeoxynucleotide from 10 to 95°C at a temperature gradient of 1°C/min. Thermal denaturation profiles are presented as first derivative plots using a window of ± 2.5°C to calculate the derivative.

### NMR spectroscopy

All NMR samples were 1.5 mM in strand d(GCATCGTT-CCCCCCTCTCTCCCCCCTTCGATGC) or d(CCCC-CCCC) in 50 mM NaCl in 100% D<sub>2</sub>O or 10% H<sub>2</sub>O/90% D<sub>2</sub>O solution. The pH was adjusted by titrating small aliquots of DCl or NaOD into the sample solution. All NMR spectra were collected on a Varian VXR500 spectrometer running at 500.1 MHz and processed on a Sun 10/30 workstation using Varian VNMR software and some software routines that were developed 'in house'. One dimensional spectra in 90% H<sub>2</sub>O/10% D<sub>2</sub>O were acquired using a 1 $\bar{1}$  echo pulse sequence (8). Two dimensional phase-sensitive nuclear Overhauser exchange spectroscopy (NOESY) data (250 ms mixing time) were acquired by the method of States *et al.* (9) with 2048×2 complex points in f<sub>2</sub> and 256×2 complex points in f<sub>1</sub>. The spectral bandwidth was 5 kHz and a recycle time of 5 s was used.

### Analytical ultracentrifugation

Sedimentation equilibrium experiments were carried out in a Beckman XL-A analytical ultracentrifuge equipped with absorbance optics. Samples and solvent (100 and 110 μl, respectively) were loaded into double sector cells with carbon filled Epon centre pieces and sedimented to equilibrium at 15°C, 40 000 r.p.m. Data were collected at equilibrium as 10 averaged scans at 260 nm. They were analysed in terms of buoyant molecular weights using the software supplied by Beckman, assuming that all species in the solution had the same partial specific volume and behaved as single ideal species. The absorbance,  $A_r$ , at any radial position,  $r$ , is related to the buoyant molecular weight  $M_b$ ,  $[M(1 - \nu\rho)]$  by the expression:

$$A_r = A_{r_0} \exp\{[\omega^2 M_b (r^2 - r_0^2)] / 2RT\}$$

where  $A_{r_0}$  is the absorbance at a reference radial position  $r_0$ ,  $\omega$  is the angular velocity,  $R$  the gas constant and  $T$  the absolute temperature.

### Circular dichroism (CD) spectroscopy

Circular dichroism spectra were recorded on a Cary 61 CD spectrometer fitted with an electro-optic modulator and interfaced to a Cleveland 286 personal computer. Oligonucleotide concentrations were in the range 50–100 μM. Cell path length was 1 mm.

### Ultraviolet absorption

Oligodeoxynucleotides were dissolved in 0.1 M sodium acetate, 10 mM NaCl, pH 5.0 or 8.0. Ultraviolet absorption spectra of 1 ml samples were recorded using a Shimadzu UV-3000 spectrophotometer. Buffer backgrounds were subtracted from all spectra.

## RESULTS

### Thermal denaturation profiles show the formation of a stable structure by CL and C<sub>8</sub> at low pH

Thermal denaturation profiles of CL at pH 8.0 and pH 5.0 are shown in Fig. 2 (A & B). Hyperchromicities and  $T_m$  values are

tabulated in Table I. At pH 8.0 CL showed a broad thermal denaturation transition around 36.5°C which showed a shift to higher  $T_m$  in the presence of 10 mM MgCl<sub>2</sub>. At pH 5.0 two sharper transitions were observed. The lower  $T_m$  transition (40.5°C) showed a shift to higher  $T_m$  in the presence of magnesium. The higher  $T_m$  transition showed little or no shift in the presence of magnesium. C<sub>8</sub> (Fig. 2C) showed two sharp thermal transitions at 37 and 61°C at acidic pH but none at alkaline pH. Both molecules also showed much greater hyperchromicity at pH 5.0 than at pH 8.0 (Fig. 2A–D, Table I).

These thermal denaturation profiles indicate the formation at low pH of a structure within the CL solution that melts at around 60°C and whose stability shows little or no dependence on the presence of Mg<sup>2+</sup>. These melting characteristics are consistent with the formation of an i-motif-like structure, which is not stabilised by Mg<sup>2+</sup>. The lower  $T_m$  transition shown by CL at both low and high pH may reflect melting of the double helical stem in CL (see Fig. 1B) as this shows substantial stabilization by Mg<sup>2+</sup>, consistent with the behaviour of Watson–Crick base paired structures (10). The strong bimodality shown by C<sub>8</sub> at pH 5 may reflect a two step melting process or the presence of two conformations in the starting mixture. The less pronounced bimodality of CL melting compared to C<sub>8</sub> may reflect more cooperative melting of the C.C<sup>+</sup> base pairs in the latter structure, possibly as a result of constraints introduced by secondary structure.

### NMR spectra support i-motif signature

Analysis of one dimensional NMR spectra of CL in 85% H<sub>2</sub>O/15% D<sub>2</sub>O at high and low pH reveals the presence of peaks centred around 15.5 p.p.m. at pH 5 (Fig. 3A) but not at pH 7.9 (data not shown). This observation is strong evidence

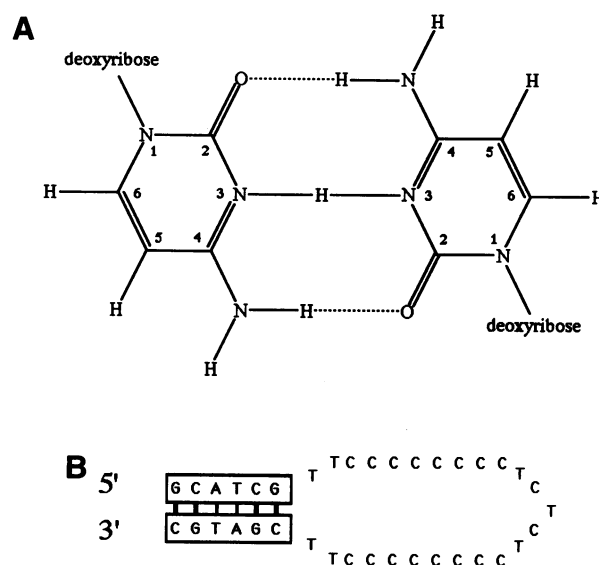


**Figure 1.** (A) Chemical structure of the C.C<sup>+</sup> base pair formed at low pH. The cytosine rings are numbered in the conventional manner. Dotted lines represent hydrogen bonds. The hydrogen bridging the two N3 positions shares its electron equally with both nitrogens. (B) Diagrammatic representation of the potential secondary structure of the CL oligodeoxynucleotide. Boxed regions of the sequence can interact to form a stem by Watson–Crick base pairing. G–C base pairs are represented by a thick line and A–T base pairs by a thin line.

for hemiprotonated C.C<sup>+</sup> base pairs (4,6). At 20°C the spectra shows 4 peaks (Fig. 3A) and as the temperature is raised to 55°C the spectrum sharpens to reveal at least 5 well-resolved peaks. The outer two peaks begin to broaden at 65°C and at 70°C all 5 are still present but somewhat broadened. The pattern of cytosine imino resonances at high temperature is similar to the pattern of cytosine imino resonances in the C<sub>8</sub> i-motif spectrum observed by Gueron and co-workers (6). Figure 3B shows the crosspeaks about the diagonal in the deoxyribose H1' region of a 2D NOESY spectrum of CL at pH 4.2. Evident are unusual inter-residue H1'–H1' crosspeaks. Such inter-residue NOE

contacts between the sugar protons are not seen in duplexes, triplexes or quadruplexes apart from the i-motif because the inter-proton distances are too great.

#### Analytical ultracentrifugation confirms that the h-dimer is a CL duplex

To test whether the above properties were due to dimer formation as opposed to the formation of higher order complexes, equilibrium sedimentation experiments were carried out at pH 5.3 and 7.9 (Fig. 4). At pH 5.3 the estimated buoyant molecular weight ( $M_b$ ) was 7500 and no evidence of heterogeneity was

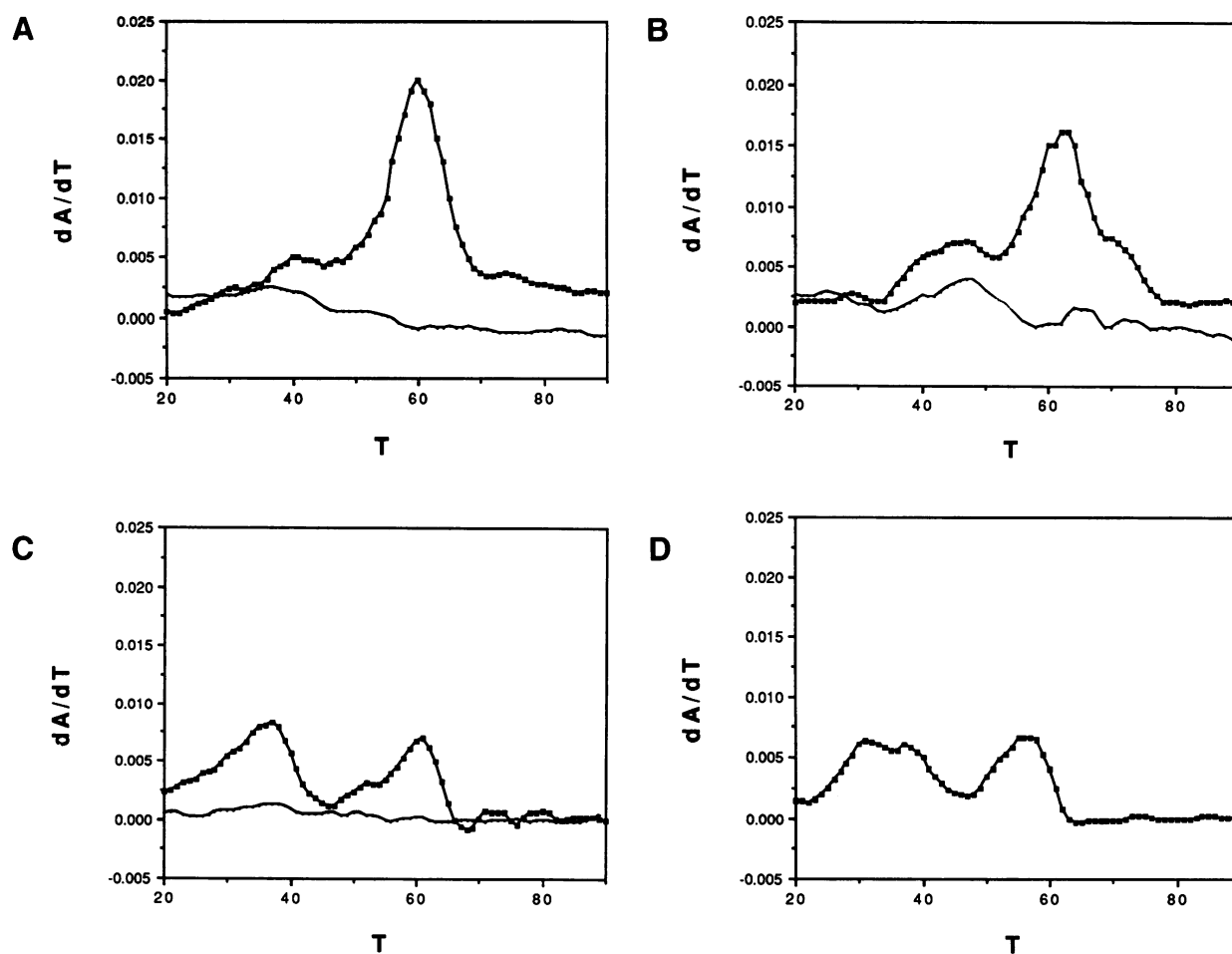


**Figure 2.** Thermal denaturation profiles of CL and C<sub>8</sub>. (A) CL in the absence of 10 mM MgCl<sub>2</sub>; (B) CL in the presence of 10 mM MgCl<sub>2</sub>; (C) C<sub>8</sub> in the absence of MgCl<sub>2</sub>; (D) C<sub>8</sub> in the presence of MgCl<sub>2</sub>. Vertical axis, rate of change of A<sub>260</sub> with temperature (dA/dT); horizontal axis, temperature (°C). Uninterrupted line, pH 8.0; dotted line, pH 5.0. Concentrations: CL, 1 μM; C<sub>8</sub>, 0.67 μM

**Table I.** Thermal denaturation and ultraviolet absorption properties of CL and C<sub>8</sub>

Oligonucleotide	pH	-Mg <sup>2+</sup>		+Mg <sup>2+</sup>		λ <sub>max</sub> (nm)
		T <sub>m</sub> (°C)	%H (%)	T <sub>m</sub> (°C)	%H (%)	
CL	5.0	40.5	26	47	24	269
		60		62.5		
C <sub>8</sub>	8.0	36.5	5	(47.5)	5	266
		37	19	31	21	
C <sub>8</sub>	5.0	52		37		273
		61		56		
		(37)	1.5	ND	ND	
	8.0			ND		269

found, whereas at pH 7.9 the estimated  $M_b$  was 3700. This gives a buoyant molecular weight ratio of 2.02 between the two pH conditions, consistent with dimer formation by CL at pH 5.3. Back calculation of the partial specific volume for CL using a molecular weight of 11 702 gave an approximate value of 0.68 ml/g, in reasonable agreement with the literature value of 0.55 ml/g (11).

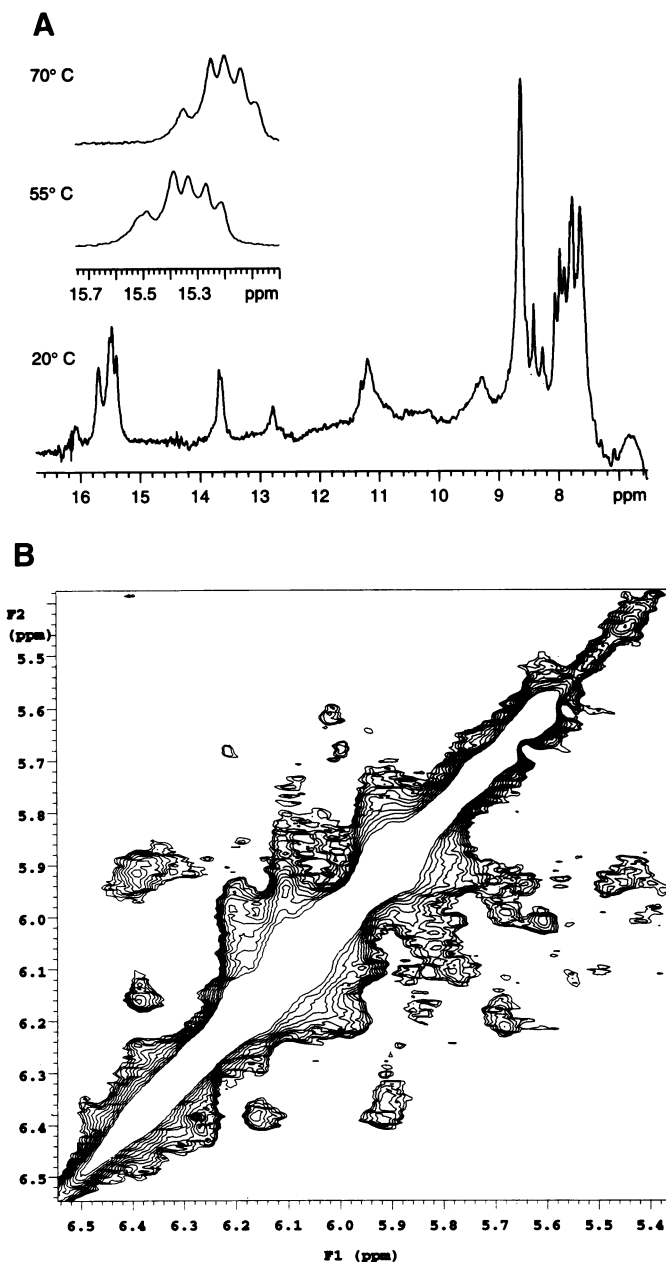


**Figure 3.** (A) 500 MHz  $^1\text{H}$  NMR spectrum of CL at 20°C. The spectrum was acquired with a 11 Echo sequence with 14 kHz spectral width, 4000 scans and a 2 s recycle delay. The  $4096 \times 2$  complex points were apodised with a 5 Hz exponential line-broadening function. (B) Expanded region of a two dimensional NOESY spectrum recorded at 25°C. Resonances corresponding to the deoxyribose H1' and cytosine H5 lie in the expanded region along the f1 and f2 axes. Several H1'–H1' crosspeaks are evident in this region. The spectral bandwidth was 5 kHz, the recycle time was 5 s, the mixing time was 250 ms and 32 scans per increment were collected. The  $2048 \times 2$  complex points in f2 and  $256 \times 2$  complex points in f1 were apodised with a shifted sinebell function.

### The CD spectrum for the h-dimer exhibits a dramatic pH dependence

At pH 7.9, the CD spectrum of CL showed a low intensity, broad peak with a maximum at 280 nm (Fig. 5). This is likely to reflect the presence of the Watson–Crick base paired double helix in the tail of the CL monomer (cf. Fig. 1B). The formation of the h-dimer at pH 5.3 in 100 mM Na acetate was accompanied by the appearance of a strong positive peak at 285 nm in the CD

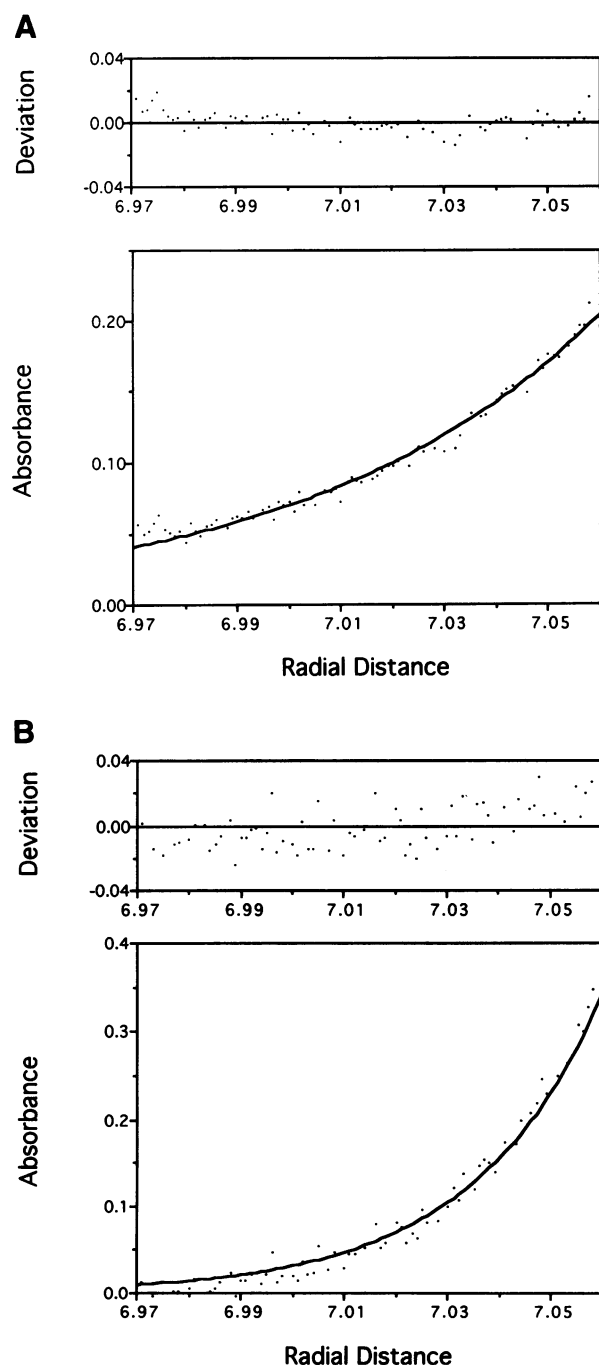


**Figure 4.** Analytical ultracentrifugation analysis of CL at pH 5.3 and 7.9. (A) 40  $\mu\text{g}/\text{ml}$  CL, pH 7.9; (B) 40  $\mu\text{g}/\text{ml}$  CL, pH 5.3. (Top) Fitted plot of  $\log(\text{solute concentration})$  vs square of radial distance; (bottom) plot of solute concentration vs square of radial distance. Radial concentration is measured in  $A_{260}$  units.

spectrum. This is consistent with the formation of an additional asymmetric structure in CL dimers at low pH. Strong positive peaks in CD spectra of tetrameric DNA structures at about 290 nm have been reported previously (12,13). In the case of tetrameric complexes of G-DNA, structures formed from linear strands have a CD spectral maxima at 265 nm (14), whereas those formed from folded strands have a maximum at  $\sim 290$  nm (13). Edwards *et al.* (15) have previously reported a CD spectral maximum at 285 nm for C.C<sup>+</sup> base paired multi-stranded DNA complexes. In retrospect these complexes based on the interaction of C<sub>4</sub>A<sub>4</sub>T<sub>4</sub>C<sub>4</sub> strands may be held together at low pH by the i-motif described by Gehring *et al.* (4).

#### Spectral shift observed on the formation of h-dimer and i-motif

Another property of CL expected to be modified by i-motif formation is its ultraviolet absorption spectrum (16). The i-motif formed by C<sub>8</sub> showed a characteristic shift of its ultraviolet absorption maximum ( $\lambda_{\max}$ ) towards longer wavelengths, having a  $\lambda_{\max}$  of 273 nm at pH 5.0 compared to 269 nm for the monomer at pH 8.0 (Fig. 6A). A similar magnitude of change of  $\lambda_{\max}$  was observed for CL, from 269 nm at pH 5.0 to 266 nm at pH 8.0 (Fig. 6B). When the pH 5.0 structures of CL or C<sub>8</sub> were melted at 90°C no further shift in UV absorption maximum was observed (data not shown).

The spectral shift observed for CL and C<sub>8</sub> at low pH is probably due to the protonation of the nitrogen at the 7 position in the cytosine ring (Fig. 1A), which alters the aromaticity of the ring. In the i-motif one hydrogen is shared equally between two cytosine rings. When melted each cytosine has an unshared proton at the N7 position, which is sufficient to maintain the spectral shift observed in the i-motif. This indicates that the aromatic ring of cytosine has the same degree of deformation in the i-motif, where protons are shared, as in the melted state, where proton sharing does not occur.

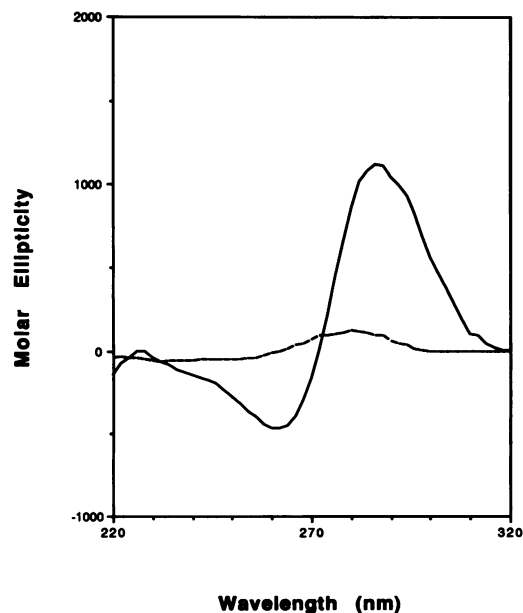


Figure 5. CD spectrum of CL. Solid line, pH 5.0; dotted line, pH 7.3. Vertical axis, molar ellipticity; horizontal axis, wavelength (nm).

## DISCUSSION

Our finding that many physical properties of CL at pH 5 are identical to those of C<sub>8</sub>, which spontaneously forms an i-motif structure at this pH (6), indicates that CL molecules, and by extension other DNA and RNA stem-loop structures with loops containing pairs of polycytidine tracts, can interact by way of C.C<sup>+</sup> base pairing to form a structure similar to the i-motif at low pH. The dimer form of CL at low pH is confirmed by analytical ultracentrifugation. Our data cannot be explained by the interaction of protonated cytosines within the loop of a hairpin, because such interaction would not result in the formation of a dimer. We describe this structure, formed between loops of stem-loop structures, as a h-dimer, to distinguish it from an i-motif formed between strands of C-rich DNA (or RNA) containing no secondary structure.

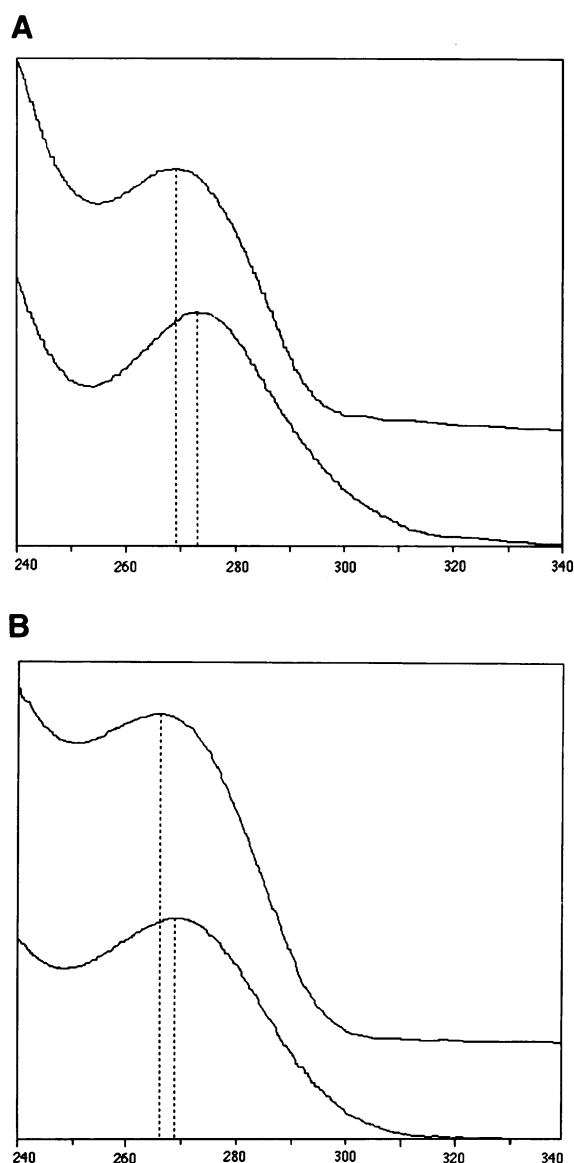


Figure 6. Ultraviolet absorption spectra of CL and C<sub>8</sub>. (A) C<sub>8</sub>. (Top) pH 8.0; (bottom) pH 5.0. (B) CL. (Top) pH 8.0; (bottom) pH 5.0. Concentrations: CL, 0.95  $\mu$ M; C<sub>8</sub>, 1  $\mu$ M. Axes: horizontal, wavelength in nm; vertical, absorbance.

The arrangement of base pairing within the i-motif is such that the interdigitating cytidine base pairs, formed between two pairs of parallel strands, lie at right angles to one another (4) (Fig. 7A). The alternative arrangement, whereby the base pairs formed by the two pairs of strands lie side by side (Fig. 7B) is not observed (4). h-Dimer formation by CL therefore requires interaction between two CL molecules in such a way as to allow an i-motif to form between the C strands of two molecules aligned in parallel. This is possible in two of the four possible conformations of a CL dimer (Fig. 7C & D). In one of these, referred to here as the *cis* 5–3 conformation, the stem regions of the monomers' secondary structure lie next to each other with the 5' end of one molecule adjacent to the 3' end of the other (Fig. 7C). The second such conformation, referred to here as the *trans* 5–5 conformation, has the monomer stem regions arranged in diametrically opposite positions within the structure with the C tracts nearest the 5' ends of the two molecules pairing with one another (Fig. 7D). Because of the conformational flexibility of the bases in the loop region, both of these structures are possible. However, the *trans* 5–5 structure would appear to be energetically favoured as it does not involve bringing the phosphates of the two double-stranded regions into close proximity. The h-dimer structure appears to be highly energetically favoured as it formed spontaneously at 0–4°C. We therefore propose that the *trans* 5–5 structure is the major dimeric conformation of the CL h-dimer at low pH.

Of particular interest is the search for possible h-dimers and i-motifs in nature. The potential for h-dimer and i-motif formation from double-stranded DNA would require special conditions to prevail. For i-motif formation *in vivo* contributions from four distinct double-stranded DNA regions would be required, while

h-dimer formation in DNA molecules would probably require circumstances under which secondary structures were extruded, for example under extreme torsional stress. Additionally, these kinds of structure may need to be stabilised by one or more proteins, as the pH range under which they are likely to be able to form [pH 3.0–6.0 by analogy with the i-motif (6)] is outside the normal physiological range. However, where they formed such structures could potentially act as protein recognition sites and might also play a role in the interaction of torsionally constrained regions of DNA in chromatin, whose folded structure could be stabilised by h-dimer formation. This is supported by the recent evidence for the i-motif being involved in the folding of cytosine-rich strands of telomeric DNA (17).

Other molecules of interest in this context are the ribosomal RNAs, which have very complex, evolutionarily conserved secondary and higher order structures (18). Despite the progress that has been made, it is clear that current knowledge cannot explain the structures of ribosomal RNA molecules completely, and in particular the long range interactions within them (18). Recent studies have shown that some long range interactions within ribosomal RNAs may be mediated by hairpin loops (19,20) raising the possibility that h-dimer-like interactions may play a role in ribosomal RNA structure. This suggestion is supported by the observation that *Escherichia coli* 23S ribosomal RNA displays a more compact conformation (higher sedimentation coefficient) at acidic pH than at neutral pH (21) and shows ultraviolet absorption shifts at low pH relative to neutral pH that have been suggested to reflect non-Watson–Crick pairing (22), although not C.C<sup>+</sup> pairing. h-Dimer formation between hairpin loops in ribosomal RNAs may therefore contribute to the stability of these molecules.

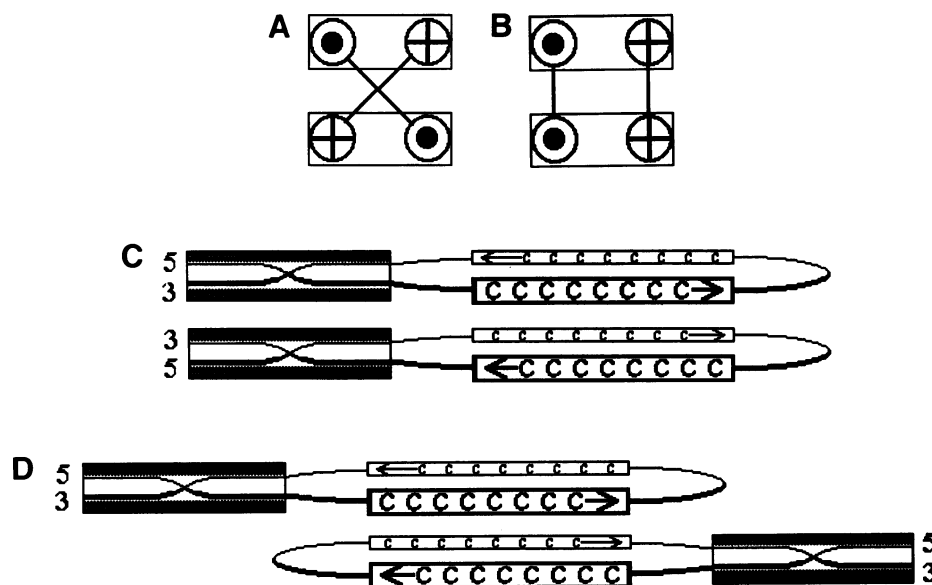


**Figure 7.** Possible conformations of the h-dimer. (A & B) Possible relative strand and pairing orientations of the loop region of CL. (A) Base pairing as in the i-motif with the directions of pairing intersecting at right angles; (B) alternative arrangement in which directions of pairing are parallel. This alternative arrangement of base pairing has been shown not to occur by NMR studies (4). Circles represent strands of the interacting poly(C) regions of the interacting loops and solid lines C.C<sup>+</sup> interactions. : 5' ∅ 3' direction out of the plane of the paper; : 5' ∅ 3' direction into the plane of the paper. Strands belonging to the same molecule are enclosed in boxes. (C & D) The two dimer conformations consistent with i-motif formation in CL. (C) *cis* 5–3 structure; (D) *trans* 5–5 structure. Polycytidine regions are boxed. 5'–3' directions of DNA strands are indicated by arrows and 5' and 3' ends of molecules are labelled. Double-stranded stems, which comprise a half turn of a helix, are indicated by shaded boxes. Figures should be seen as perspective drawings, with shaded parts of strands and large lettering towards the reader and unshaded parts with small lettering away.

Tests for the presence of h-dimer and i-motif structures in biological macromolecules could make use of both biophysical and biochemical approaches. In principle the most definitive biophysical test for the presence of i-motifs is the appearance of NMR resonances in the 15.5–16 p.p.m. region at low pH and the appearance of inter-residue sugar–sugar crosspeaks in NOESY spectra. However, such an approach is not likely to be useful as detailed NMR analysis of very large molecules is impractical. It should be noted that C.C<sup>+</sup> base pairs in tetrameric structures other than the i-motif has a cytidine imino resonance slightly less than 15 p.p.m. (23,24). A more practical test may be the appearance of a strong CD peak around 285 nm or a strong thermal melting transition above 60°C at low pH. An alternative assay for h-dimer or i-motif formation would be reaction with antibodies to these structures. In addition, if specific proteins can be positively identified that interact with these structures, such proteins might be used in affinity assays.

## ACKNOWLEDGEMENTS

We thank Barry Osmond for his support, Les Lane for helpful discussion and encouragement, Peter Jeffrey for assistance with analytical ultracentrifugation and Elisabeth Owen for assistance with the CD spectrometry. This work benefited from the use of equipment at the NMR facility at the Australian National University.

## REFERENCES

1. Smith, F.W. & Feidon, J. (1992) *Nature* **356**, 164–168.
2. Wang, Y. & Patel, D.J. (1992) *Biochemistry* **31**, 8112–8119.
3. Kang, C., Zhang, X., Ratliff, R., Moyzis, R. & Rich, A. (1992) *Nature* **356**, 126–131.
4. Gehring, K., Leroy, J.-L. & Guéron, M. (1993) *Nature* **363**, 561–565.
5. Patel, D.J. (1993) *Nature* **363**, 499–500.
6. Leroy, J.-L., Gehring, K., Kettani, A & Guéron, M. (1993) *Biochemistry* **32**, 6019–6031.
7. Maher, L.J. (1992) *BioEssays* **14**, 807–815.
8. Sklenar, V. & Bax, A. (1987) *J. Magn. Reson.* **74**, 469–479.
9. States, D.J., Haberkorn, R.A. & Ruben, D.J. (1982) *J. Magn. Reson.* **48**, 286–292.
10. Record, M.T. (1975) *Biopolymers* **14**, 2137–2158.
11. Bloomfield, V.A., Crothers, D.M. & Tinoco, I. (1974) *Physical Chemistry of Nucleic Acids* (Harper & Son, New York, NY) p. 222.
12. Scaria, P.V., Shire, S.J. & Shafer, R.H. (1992) *Proc. Natl. Acad. Sci. USA* **89**, 10336–10340.
13. Jin, R., Breslauer, K.J., Jones, R.A. & Gaffney, B. (1990) *Science* **250**, 543–546.
14. Jin, R., Gaffney, B.L., Wang, C., Jones, R.A. & Breslauer, K.J. (1992) *Proc. Natl. Acad. Sci. USA* **89**, 8832–8836.
15. Edwards, E.L., Patrick, M.H., Ratliff, R.L. & Gray, D.M. (1990) *Biochemistry* **29**, 828–836.
16. Van Holde, K.E. (1971) *Physical Biochemistry* (Prentice Hall, Eaglewood Cliffs, NJ).
17. Leroy, J.-L., Guéron, M., Mergny, J.-L. & Helene, C. (1994) *Nucleic Acids Research* **22**, 1600–1606.
18. Gutell, R.R., Power, A., Hertz, E.J. & Stormo, G.D. (1992) *Nucleic Acids Research* **20**, 5785–5795.
19. Jaeger, L., Michel, F. & Westhof, E. (1994) *J. Mol. Biol.* **236**, 1271–1276.
20. Woese, C.R., Winker, S. & Gutell, R.R. (1990) *Proc Natl Acad Sci USA* **87**, 8467–8471.
21. Nisbet, J.H. & Slayter, H.S. (1975) *Biochemistry* **14**, 4003–4010.
22. Revzin, A., Neumann, E. & Katchalsky, A. (1973) *J. Mol. Biol.* **79**, 95–114.
23. Radhakrishnan, I., Gao, X., de los Santos, C., Live, D. & Patel, D.J. (1991) *Biochemistry* **30**, 9022–9030.
24. Hardin, C.C., Corregan, M., Brown II, B.A. & Fredrick, L.N. (1993) *Biochemistry* **32**, 5870–5880.